Journal of CO2 Utilization 62 (2022) 102085

Contents lists available at ScienceDirect

Journal of CO2 Utilization

journal homepage: www.elsevier.com/locate/jcou

Improvement of CO_2 absorption and inhibition of NH_3 escape during $CaCO_3$ precipitation in the presence of selected alcohols and polyols

Natalia Czaplicka [a,*], Dominik Dobrzyniewski [a], Szymon Dudziak [a], Chunqing Jiang [b], Donata Konopacka-Łyskawa [a]

[a] Department of Process Engineering and Chemical Technology, Faculty of Chemistry, Gdansk University of Technology, Narutowicza 11/12, 80-233 Gdansk, Poland
[b] Natural Resources Canada, Geological Survey of Canada, 3303–33 Street NW, Calgary, Alberta T2L 2A7, Canada

ARTICLE INFO

Keywords:
CO2 utilization
CO2 absorption
Calcium carbonate
Carbonation
Ammonia escape, inhibitors

ABSTRACT

This research aims to investigate the effect of selected organic substances containing hydroxyl groups on the reduction of NH_3 escape and the improvement of CO_2 capture during the precipitation of calcium carbonate by carbonation method using post-distillation liquid from the Solvay process and gas stream containing CO_2 in the amount corresponding to the exhausted gases produced by the combustion of fossil fuels. Glycerol, ethylene glycol (EG), methanol, isopropanol, pentaerythritol, and neopentyl glycol (NPG) were used as ammonia escape inhibitors. The addition of NPG has been shown to result in the highest reduction of NH_3 escape (83.1%) and the highest CO_2 capture efficiency (86.1%). During the proposed $CaCO_3$ precipitation with NPG, 98.7% of the NH_3 initially introduced into the reaction mixture remains in the solution. Furthermore, the features that should be taken into account when introducing various alcohols and polyols for capturing NH_3 and CO_2 in the calcium carbonate precipitation via the carbonation method have been discussed.

1. Introduction

Increased level of CO_2 in the atmosphere is widely considered the dominant cause for the global warming observed during the past decades and the catastrophic climate conditions experienced by human beings in the past years [1,2]. This understanding has prompted extensive academic research and exploratory industrial practices in the area of carbon capture, utilization and storage (CCUS) in order to reduce the input of anthropogenic CO_2 into the atmosphere [3]. Among the various means of CCUS, CO_2 mineralization by reacting the greenhouse gas with certain divalent metal minerals such as basaltic and ultramafic rocks to form solid carbonates has the potential to store CO_2 permanently either in the geological formations, on the ocean floors or on the land surface [4–6]. Of the CO_2 mineralization approaches, *ex situ* and surficial CO_2 mineralization using industrial waste by-products and mine tailings as the source of divalent cations are of special interest and benefit as the processes not only remove and store CO_2 but also mitigate environmental issues associated with the waste material/streams and produce valuable mineral products [5]. Moreover, the implementation of such a technology allows production plants to not only obtain financial benefits from the sale of precipitated carbonates, but also reduce expenses for environmental pollution [7]. Amongst the various industrial wastes capable of solidifying CO_2, waste streams from the Solvay processes and petroleum brines from the oil and gas industries are among the best candidates due to their high contents of total dissolved solids (TDS). For example, flowback and produced water (FPW) from the Duvernay shale and Montney tight reservoir hydraulic fracturing (HF) operations in Western Canada can have on average 230 g/L of TDS in the forms of sodium, potassium, calcium, magnesium and strontium chlorides [8]. High levels of TDS have also been reported in FPW from some active unconventional hydrocarbon production regions in US, UK and Poland [9]. On the other hand, the post-distillation liquid from Solvay process for sodium carbonate production contain about 112 g/L $CaCl_2$ and 56 g/L NaCl [10–12]. Soda plants using the Solvay method store the post-distillation waste liquid mainly in landfills called white seas or discharge it directly into the sea. Such an approach poses a serious threat to the environment as it results in increased salinity of the surrounding soil and groundwater [10]. Therefore, an important environmental issue is to find alternative management methods for efficient recycling of this type of problematic, highly saline waste.

Recently, there have been increasing research efforts on the use of calcium-rich waste as substrates for the production of $CaCO_3$ by the

---

* Corresponding author.
E-mail address: natalia.czaplicka@pg.edu.pl (N. Czaplicka).

https://doi.org/10.1016/j.jcou.2022.102085
Received 19 April 2022; Received in revised form 26 May 2022; Accepted 7 June 2022

carbonation method using waste gaseous stream containing CO_2 [12,13]. This method requires the use of so-called absorption promoters. In the industry, the most common CO_2 absorbents are ethanolamines such as monoethalamine (MEA), diethanolamine (DEA), and triethanolamine (TEA) [14]. These amines have a high CO_2 absorption capacity and thermal stability, and are non-volatile and inexpensive; however, the biggest problem with their use is the high cost associated with their regeneration after the absorption process and their strong corrosivity to the equipment [15]. Currently, one of the most popular alternatives to ethanolamines is an aqueous solution of ammonia, which is reflected in the increasing amount of research in this matter [16–19]. Compared with the ethanolamine techniques, the ammonia solution approaches are characterized by a higher CO_2 capture capacity, lower price, and non-degradation in the presence of O_2 and SO_2 [20]. For example, the absorption capacity of ammonia is 1.2 kg CO_2/kg NH_3, while in the case of MEA it is 0.4 kg CO_2/kg MEA [20]. Moreover, ammonia solution have the potential to capture many acid gases besides CO_2 present in exhaust gases, i.e., SO_x and NO_x. More importantly, processes using NH_3 solutions have low energy demand [21,22]. Despite the many advantages, the biggest problem with using NH_3 for CO_2 absorption is its high volatility [23]. The intrinsically high volatility of ammonia causes its escape from the aqueous solution, lowering its concentration in the solution and thus reducing the efficiency of the CO_2 capture process. Consequently, this increases the amount of NH_3 needed to absorb a given amount of CO_2 [23].

Many methods have been proposed to prevent the escape of ammonia from the solution. One of them is the addition of the so-called ammonia escape inhibitors to the solution [24,25], which is a promising solution for capturing CO_2 in the $CaCO_3$ carbonation process. Our previous research compared organic and inorganic ammonia escape inhibitors and determined their influence on the characteristics of the obtained calcium carbonate [26]. None of the tested inorganic inhibitors (e.g., $ZnCl_2$, $CoCl_2$, and $CuCl_2$) was found to show any improvement in CO_2 sequestration. Moreover, the precipitated $CaCO_3$ particles often contained colored ammonia complexes of the metals used when inorganic ammonia escape inhibitors were added to the solution [26]. Another important disadvantage of applying inorganic inhibitors is the potential precipitation of hydroxide or carbonate of the added divalent cations in an alkaline solution [23]. Thus, it is obvious that organic substances are more suitable for this type of application. One such group of organic inhibitors are alcohols and polyols due to the presence of hydroxyl groups in their molecules capable of forming hydrogen bonds with ammonia molecules in an aqueous solution [27]. There are reports in the literature on the use of ethanol [28,29], glycerol [30,31], and ethylene glycol [30,32] as ammonia escape inhibitors for the purpose for CO_2 capture. Furthermore, the alcohol-water mixtures are popular additives in the $CaCO_3$ precipitation process, because the addition of alcohols may have a chemical effect on the aqueous solution by decreasing the solubility of $CaCO_3$ and thus increasing its supersaturation tendency [33]. The use of a small (several percent) addition of alcohols or polyols also has advantages from an economic point of view. Due to the low prices of this type of solvents (e.g. ethylene glycol 1.5 \$/kg, glycerol 1 \$/kg, methanol and isopropanol 3–5 \$/kg), such a solution practically does not increase the cost of the process. Moreover, the use of expensive equipment is not required, and the introduction of such a solution allows the use of existing equipment without costly modifications. Finally, while the addition of an alcohol or polyol greatly improves the selectivity of the absorbent, it thereby reduces the amount of solvent circulation and energy consumption, and then lowers the operating costs [23].

This research is a continuation of previous studies on carbonation using post-distillation liquid from the Solvay process as the source of calcium and a waste gas stream with a composition typical of the exhausted gases from fossil fuel combustion as the source of CO_2. In addition to the previously characterized organic substances glycerol and ethylene glycol, two alcohols (methanol and isopropanol) and two polyols (pentaerythritol and neopentyl glycol) are used in the present study to compare their ability to reduce the escape of ammonia from the solution. The second aim of the research is to determine the influence of the various additives on CO_2 capture during the calcium carbonate precipitation process.

2. Materials and methods

2.1. Reagents

Reagents used in this work include anhydrous calcium chloride (POCH, Poland), sodium chloride (P.P.H. STANLAB, Poland), glycerol (POCH, Poland), ethylene glycol (≥99.0%, POCH, Poland), methanol (POCH, Poland), isopropanol (POCH, Poland), pentaerythritol (Sigma-Aldrich, USA), neopentyl glycol (NPG: Sigma-Aldrich, USA), 25% aqueous ammonia solution (POCH, Poland), di-sodium wersenate, 0.1 mol/L solution (Chempur, Poland), buffer solution pH 10 ± 0.05 (Chempur, Poland), eriochrome black T (Chempur, Poland), and carbon dioxide (Linde Gas, Poland). All reagents were of analytical grade and were used without further purification. All solutions were prepared using water obtained by reverse osmosis.

2.2. Precipitation of calcium carbonate

The precipitation process was carried out using gas-liquid carbonation method at room temperature (295 K) and atmospheric pressure (1013 hPa) in a closed tank reactor with a total volume of 0.5 dm^3. Gaseous CO_2 was continuously supplied into the reaction system in a mixture with air through a porous glass plate. Gas mixing occurred during the flow and before it was supplied into the liquid phase. The detailed procedure for supplying the gas mixture to the system and the description of the experimental setup are described in Section 2.4. The reaction time was 1.5 h, while the initial reactant mixtures (0.3 dm^3) were a model post-distillation liquid from the Solvay process (an aqueous solution containing 112 g/dm^3 of $CaCl_2$ and 56 g/dm^3 of NaCl) without (as control) and with the addition of tested alcohols and polyols. The concentration of glycerol, ethylene glycol, methanol and isopropanol in the reactant mixture equals 1% (v/v), while the concentration of solid pentaerythritol and neopentyl glycol was 1% (w/w). The molar ratio of ammonia to calcium ions in the initial solutions was 2:1 (NH_3 concentration of 2.02 mol/L). The ammonia was added to the reaction mixture as a 25% aqueous solution. Initial and final pH of the reaction mixture were measured using composite electrode (ERH-111 type, HYDROMET, Poland) connected to the pH meter. The final Ca^{2+} concentration in the reaction mixture was determined by a complexometric titration of collected samples with EDTA. Ammonia and CO_2 concentrations in outlet stream were measured using sensors described in Section 2.3. The processes of CO_2 absorption in an aqueous ammonia solution of the same concentration and under the same conditions as the precipitation process were also performed. The obtained calcium carbonate particles was filtered and washed with water and methanol, and dried for 24 h at 90 °C. X-ray diffraction (XRD) analysis with Cu-Kα radiation was applied to confirm that the obtained product is in the form of calcium carbonate and to determine its polymorphic composition. The analysis was carried out using a MiniFlex 600 diffractometer (Rigaku, Tokyo, Japan) at room temperature, at 0.2° scan rate and 2θ angle range of 10–80°. Diffractograms were optimized using a pseudo-Voight function, and ICDD database was applied for phase identification of the precipitated samples.

2.3. CO_2 and NH_3 gas flow measurement

In order to monitor and control the process, a matrix comprised of two commercially available gas sensors was constructed for determine the concentrations of CO_2 and NH_3 in the outlet gas stream from the reaction system. Table 1 presents the basic information about the gas

Table 1
Basic characteristics of the sensors used.

Sensor Type	Model	Target Gas
Electrochemical	SGX-4NH3–1000	Ammonia
Nondispersive Infrared Sensor	DFrobot Gravity UART	Carbon dioxide

sensors used.

The infrared carbon dioxide gas sensor enables the detection of target gas in a wide effective range from 0 to 5000 ppm. It is characterized by high sensitivity, high resolution, good stability, low power consumption and quick response. This sensor also provides a digital output proportional to the concentration of carbon dioxide, which is temperature compensated and thus the output signal is completely linearized. The ammonia sensor used belongs to the group of electrochemical sensors. In this type of sensors, the target gases undergo a chemical reaction (oxidation or reduction) at an electrode, resulting in a current directly proportional to the gases concentration. Electrochemical ammonia gas sensor (SGX-4NH3–1000), manufactured by Amphenol Company, makes it possible to detect ammonia in concentrations ranging from 0 to 1000 ppm. Moreover, operation and use of the sensors is not complicated as they support UART communication mode and analog output. Sensor calibrations can be found in Supplementary Materials (Fig. S1 and Table S1).

2.4. *Gas sensor array measurement*

Gas sensor array experimental setup is presented in Fig. 1. The total gas flow rate was 500 mL/min with carbon dioxide and air flow rates being controlled by separate mass flow controllers. The volumetric flow rate of carbon dioxide was controlled by a RED-Y GSC-B9SS-BB23 (Voegtlin, Switzerland) flowmeter (MFC 3) and was equal to 75 mL/min so that the concentration of carbon dioxide in the flowing gas mixture was 15% by volume (stream containing CO_2 in the amount corresponding to the exhausted gases produced by the combustion of fossil fuels). Airflow was controlled using RED-Y GSC-C9SS-BB26 (Voegtlin, Switzerland) flowmeter (MFC 2) and amounted to 425 mL/min. The residual gas stream after passing through the reaction glass vessel containing the post-distillation liquid from the Solvay process was directed to the mixing chamber in an exact volume. In the mixing chamber, this residual gas stream was mixed with an air stream whose volumetric flow rate was 150 L/h and controlled by a flowmeter RED-Y GSC-C9SS-BB26 (MFC 1). This allowed the residual gas to be diluted to a sufficiently low level before being directed to the sensor chambers. The volume of the gas stream dispensed into the chamber was controlled by a rotation speed of the diaphragm pump. The pulse width modulation module (PWM) was responsible for regulating the supply voltage delivered to the pump motor, fluctuations of which directly affect the pump speed and thus the flow rate. The sensors were housed in separate Teflon gas chambers that provide individual gas environment for each sensor and parallel gas flow. Thanks to this, it was possible to limit the adsorption and avoid undesirable chemical transformation of gaseous substances. Sensor signals were recorded using an analog-to-digital converter ADS1115 (Texas Instruments, USA) and processed by means of dedicated software. All manufacturer's requirements were taken into account when the electrical circuits for each sensors were prepared. The custom-built system was controlled automatically by the Arduino MEGA 2560 Rev3 control module.

The in-house software allowed for calculation of ammonia and carbon dioxide concentrations at the outlet of the reactor. Knowing the volumetric flow rate, the total number of moles of ammonia and CO_2 that left the system while the process was running was then calculated.

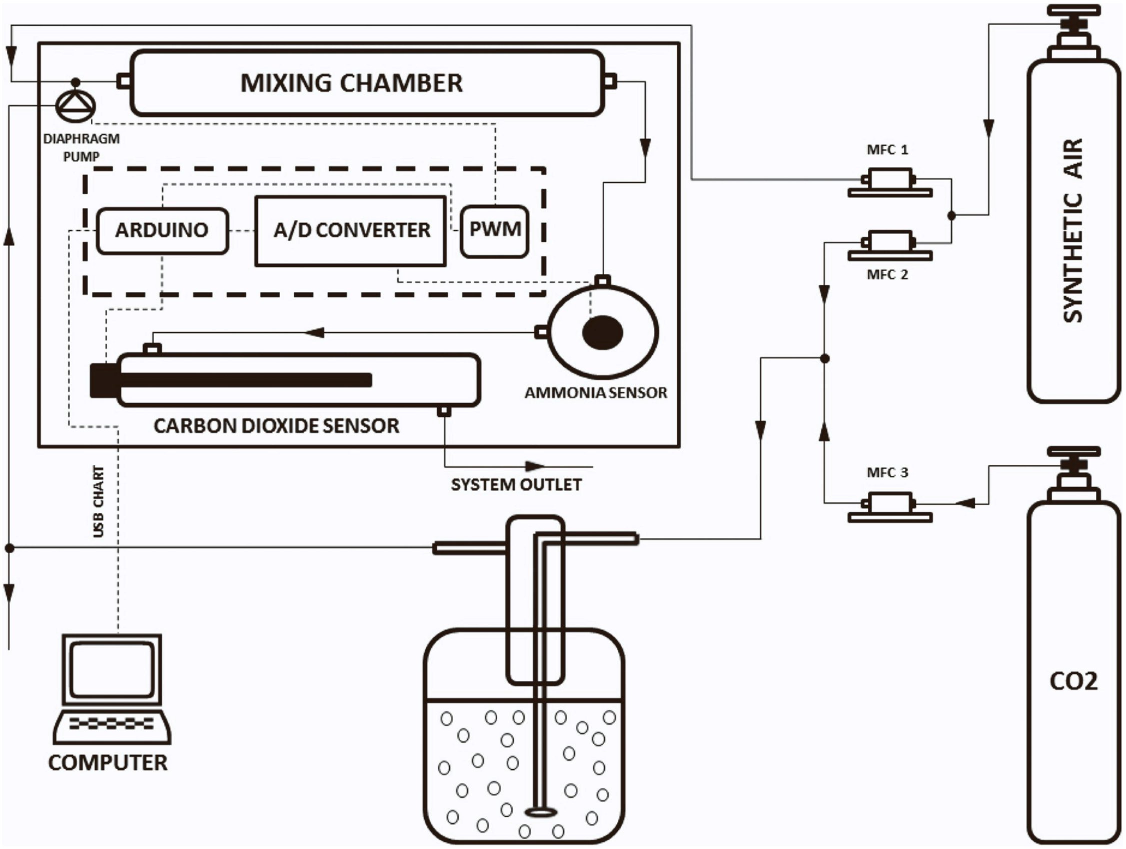

Fig. 1. Experimental setup scheme.

2.5. Interactions and hydrogen bonding calculations

Interactions and H-bonding between the studied alcohols and the $NH_4^+/NH_3/H_2O$ species were investigated computationally at the density functional theory (DFT) level using B3LYP hybrid functionals and the D3BJ dispersion correction, as implemented in the Orca 4.2.1. software package [34]. During the calculations, geometries of all structures, isolated and bonded, were optimized to an energy threshold of 10–8 Ha and the energy difference between isolated substrates and bonded complexes were calculated to compare bonding effect for different species. In case of pentaerythritol, NPG, glycerol and ethylene glycol, two geometries, both single and 2 H-bonds, were investigated to better compare possible effects. During all calculations, conductor-like polarizable continuum model (CPMC) of solvation was introduced to account for the solvent present in the real process.

3. Results and discussion

3.1. The course of the precipitation and adsorption processes

The process of calcium carbonate precipitation was carried out using post-distillation liquid from the Solvay process and a gas stream containing CO_2 with a composition corresponding to the exhausted gases produced by the fossil fuel combustion (15% vol.). Ammonia was used as a CO_2 absorption promoter for the calcium carbonate precipitation, because an aqueous NH_3 solution is one of the most popular alternatives to ethanolamines as CO_2 absorbents. The processes of CO_2 absorption in a pure aqueous ammonia solution of the same concentration and under the same conditions as the carbonate precipitation process were also performed for comparison with the precipitation processes. Figs. 2 and 3 present the gas sensor recorded graphs showing changes in the concentrations of ammonia and carbon dioxide detected in the outlet gas stream during the course of the carbonation and absorption processes for different additives used. The actual amounts (in moles) of CO_2 and NH_3 that have escaped from the solution are included in Tables 2 and 3, respectively. It is generally accepted that the major steps in the chemical absorption of CO_2 capture by an aqueous ammonia solution can be described by reactions shown in Eqs. (1)–(7) [35,36]. The first is the production of an unstable carbamic acid, which rapidly converts to ammonium carbamate (Eq. (1)). This is followed by the hydrolysis of the ammonium carbamate (Eq. (2)) and the hydrolysis of the ammonia (Eq. (3)). At the same time, a complex equilibrium of the ions and reactions described in Eqs. (4)–(7) takes place in the solution. This results in the formation of bicarbonate and carbonate ions.

$$CO_{2(g)} + 2NH_{3(aq)} \rightarrow H_2NCOO^-_{(aq)} + NH^+_{4(aq)} \tag{1}$$

$$H_2NCOO^-_{(aq)} + NH^+_{4(aq)} + 2H_2O \rightarrow NH_4HCO_{3(aq)} + NH_3 \bullet H_2O_{(aq)} \tag{2}$$

$$NH_{3(aq)} + H_2O_{(aq)} \leftrightarrow NH^+_{4(aq)} + OH^-_{(aq)} \tag{3}$$

$$NH_4HCO_{3(aq)} \leftrightarrow NH^+_{4(aq)} + HCO^-_{3(aq)} \tag{4}$$

$$(NH_4)_2CO_{3(aq)} \leftrightarrow 2NH^+_{4(aq)} + CO^{2-}_{3(aq)} \tag{5}$$

$$OH^-_{(aq)} + HCO^-_{3(aq)} \leftrightarrow CO^{2-}_{3(aq)} + H_2O \tag{6}$$

$$CO^{2-}_{3(aq)} + CO_{2(g)} + H_2O \leftrightarrow 2HCO^-_{3(aq)} \tag{7}$$

When analyzing changes in the amount of ammonia over time, it can be seen that the graphs are very similar regardless of the additive used. There is a sharp increase in the beginning, followed by a slow decline. Initially, a high concentration of free NH_3 is in the reaction mixture, and as the CO_2 absorption process progresses, more ammonia is consumed by the reactions shown in Eqs. (1)–(7). This results in a reduction in the amount of free NH_3 in the absorption mixture, which in turn reduces the amount of ammonia that escapes from the solution [37].

The system used in these tests is semi-batch, i.e. the reactor is filled with a portion of liquid, and the gas phase flows through the reactor continuously. During carbonation, some of the reactants in the liquid phase (Ca^{2+} and NH_3/NH_4^+) are consumed, while CO_2 is continuously supplied to the reactor. Therefore, immediately after starting the gas flow through the reactor, NH_3 is desorbed into the gas stream, however, due to the reaction between NH_3 and CO_2, the amount of free NH_3 in the solution decreases, therefore its desorption to the gas stream flowing through the reactor is reduced.

In the case of CO_2 absorption in ammonia-water systems, very similar courses of the CO_2 concentration curves have been observed. While in the case of changes in CO_2 concentration, after about 1 h of the precipitation process, a rapid increase in the amount of CO_2 in the outlet stream occurs for reaction systems with the addition of methanol, isopropanol and neopentyl glycol. This is likely due to the drop of the pH of the solutions at that point. The final pH values for precipitation systems containing these three inhibitors reached the values of 7.89, 7.57, and 7.43, respectively (Table 4). When the solution reaches a pH below 8, the amount of free CO_2 in the solution increases while the amount of CO_2 in dissociated form decreases, and this favors the escape of CO_2 from the solution [38].

The presence of CO_2 in the gas outlet stream from the reactor is the result of the kinetics of CO_2 absorption and its reaction with ions present in the solution. Research on the kinetics of CO_2 absorption in aqueous ammonia solutions indicated a similar course of the molar fraction of CO_2 in the outlet gas [39]. In pure ammonia solutions, three periods were found: initial period, stable period, and rising period. In the first period, after activating the gas (CO_2-air mixture) supply, CO_2 is absorbed in the alkaline solution and then reacts with NH_4^+ ions. The rapid increase in CO_2 concentration observed may be the result of the kinetics of CO_2 absorption in the ammonia solution. Subsequently, for most systems there is a stable period, which is characterized by a stabilized CO_2 concentration in the exhaust gas or its slight increase. The last period is the rising period in which the CO_2 concentration in the off-gas increases significantly.

3.2. Ammonia escape inhibition

Based on the results obtained, percentage reduction of NH_3 escape (η) was calculated using the Eq. (8) and results obtained are shown in Table 2.

$$\eta = \frac{n_0 - n_A}{n_0} \bullet 100\% \tag{8}$$

where n_0 is the total number of NH_3 moles escaping from the reaction mixture without additives (control), and n_A is the total number of NH_3 moles escaping from the reaction mixture with selected additives. Generally, all tested additives contain the hydroxyl groups that can combine with the free NH_3 through hydrogen bonding, thereby inhibiting its evaporation from the solution. In calcium carbonate precipitation processes with all additives used, more than 97% of the NH_3 initially introduced into the reaction mixture remains in the solution, higher the 92.5% capture efficiency for the precipitation system without additives (Fig. 4). The NH_3 salting-out effect by the electrolytes is quite obvious for the post-distillation liquid compared with the ammonia solution, because the solubility of NH_3 in water is reduced in the presence of dissolved inorganic salts [40]. Usually, the effect of the salt addition on the solubility has been attributed to the greater attraction between the ions and the water molecules than between the gas molecules. Electrolytes with small ions can influence on the organization of the structure of water. Therefore, interactions between the ions and water molecules should decrease the number of ‘free’ water molecules available to dissolve the gas [41]. The results obtained show that the addition of selected organic compounds inhibits the escape of ammonia by the

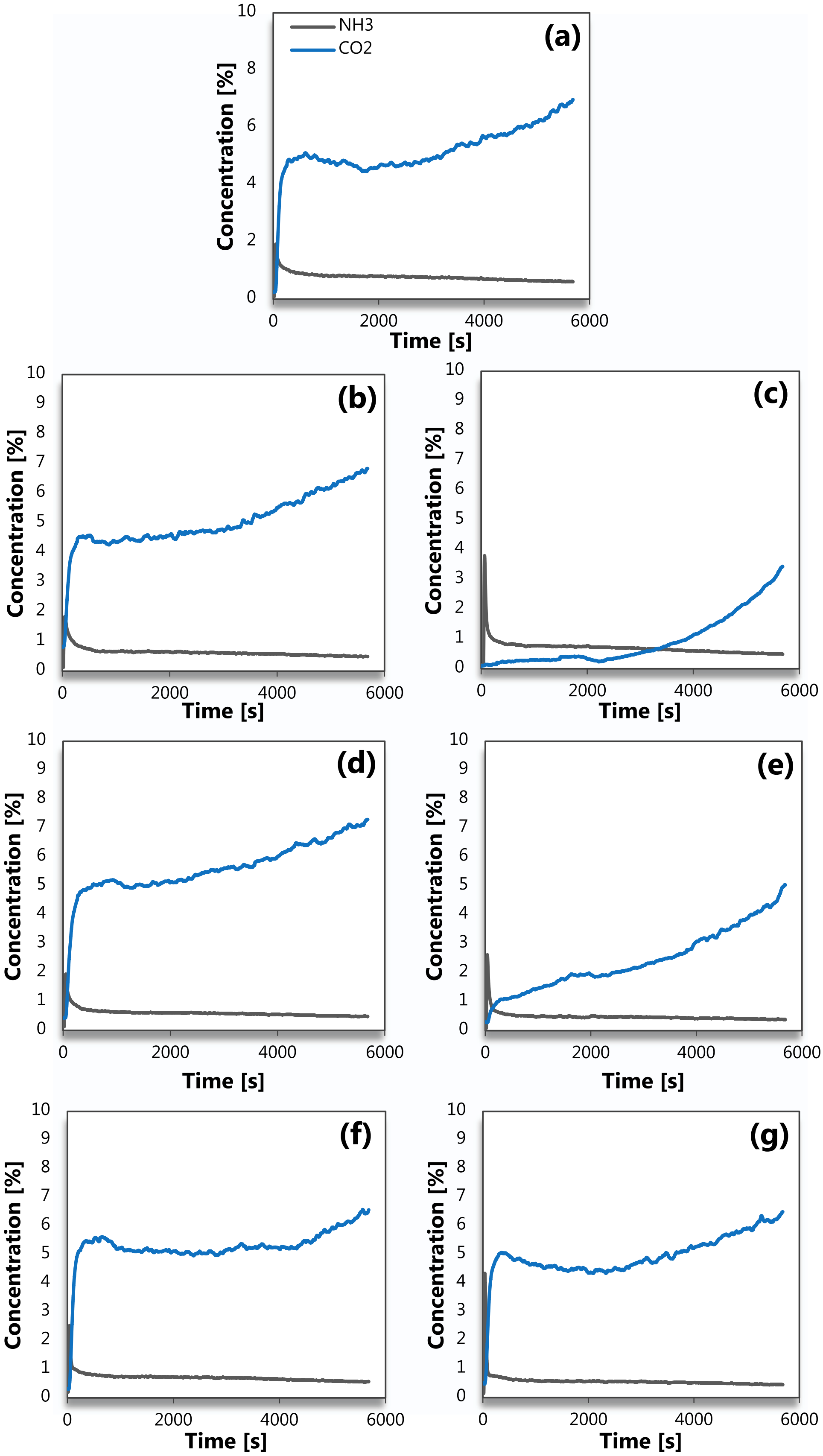

Fig. 2. Variation in the concentrations of NH_3 and CO_2 during the course of CO_2 absorption in aqueous ammonia solution (a) without additives and in the presence of (b) methanol, (c) isopropanol, (d) ethylene glycol, (e) neopentyl glycol, (f) glycerol, and (g) pentaerythritol.

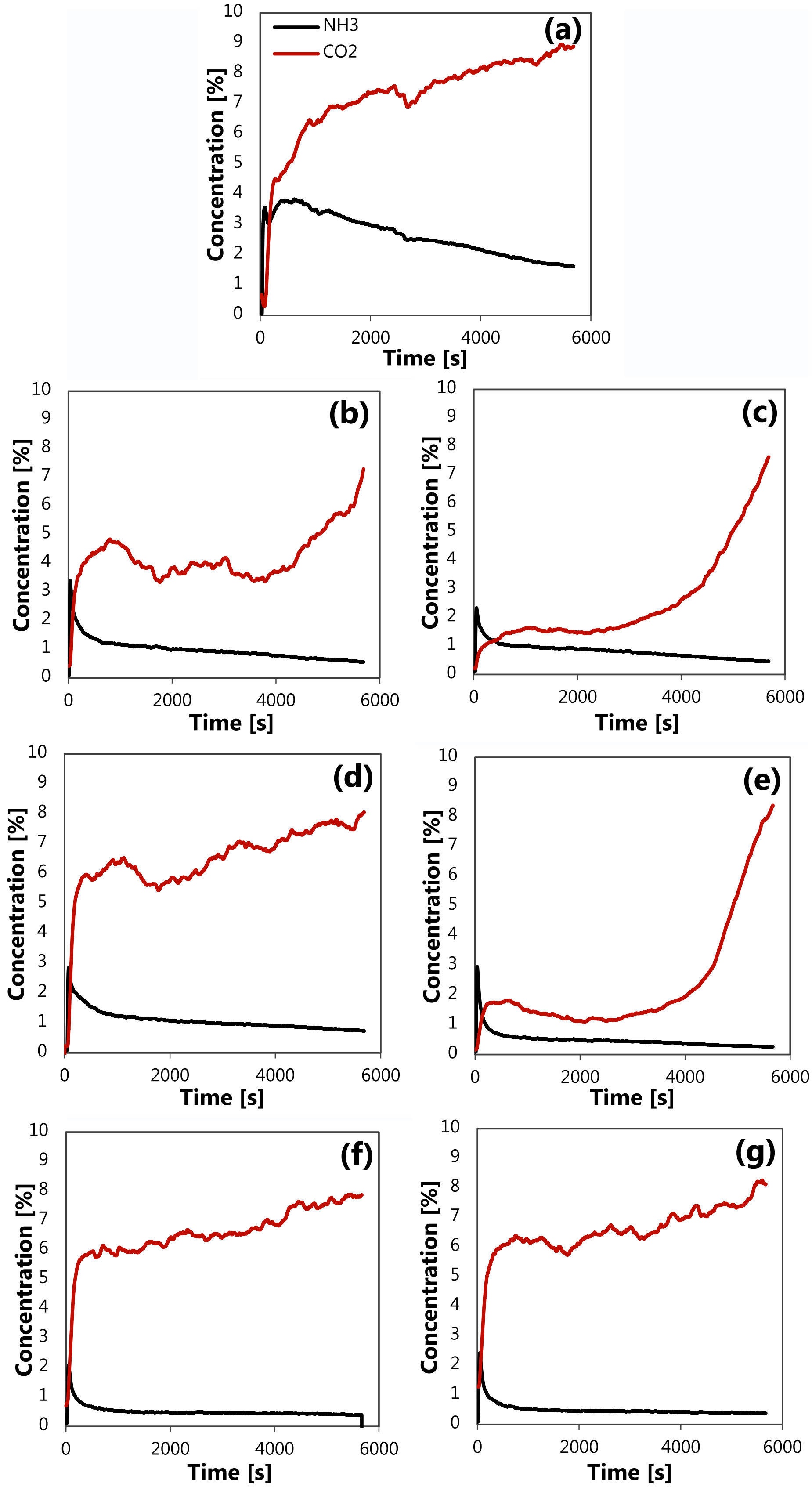

Fig. 3. Variation in the concentrations of NH_3 and CO_2 during the course of $CaCO_3$ precipitation (a) without additives and in the presence of (b) methanol, (c) isopropanol, (d) ethylene glycol, (e) neopentyl glycol, (f) glycerol, and (g) pentaerythritol.

Table 2
The amount of NH_3 that escaped from the solution during the process and the percentage reduction of NH_3 escape (initial moles of $NH_3 = 0.606$).

Experiment	NH_3 escape [mol]		Reduction of NH_3 escape [%]	
	Absorption system$^{1)}$	Precipitation system$^{2)}$	Absorption system$^{1)}$	Precipitation system$^{2)}$
Control (no additives)	0.0128	0.0456	–	–
1% vol. glycerol	0.0117	0.0085	8.6%	81.4%
1% vol. EG	0.0101	0.0183	21.1%	59.9%
1% vol. MeOH	0.0105	0.0160	18.0%	64.9%
1% vol. iPrOH	0.0112	0.0132	12.5%	71.1%
1% wt. pentaerythritol	0.0094	0.0084	26.6%	81.6%
1% wt. NPG	0.0078	0.0077	39.1%	83.1%

[1] Aqueous ammonia solution
[2] Post-distillation liquid from the Solvay process

Table 3
The amount of CO_2 that escaped from the solution during the process and the CO_2 capture efficiency.

Experiment	CO_2 escape [mol]		CO_2 capture efficiency [%]	
	Absorption system$^{1)}$	Precipitation system$^{2)}$	Absorption system$^{1)}$	Precipitation system$^{2)}$
Control (no additives)	0.0875	0.1259	68.6%	54.9%
1% vol. glycerol	0.0886	0.1105	68.2%	60.4%
1% vol. EG	0.0937	0.1116	66.4%	60.0%
1% vol. MeOH	0.0701	0.0842	74.9%	69.8%
1% vol. iPrOH	0.0151	0.0419	94.6%	85.0%
1% wt. pentaerythritol	0.0824	0.1104	70.5%	60.4%
1% wt. NPG	0.0406	0.0393	85.4%	86.1%

[1] Aqueous ammonia solution
[2] Post-distillation liquid from the Solvay process

Table 4
Ca^{2+} ions consumption ($[Ca^{2+}]$), initial and final pH of reaction mixtures (pH_i, pH_f).

Experiment	pH_i	pH_f	Consumed Ca^{2+} [mol/dm^3]	% Ca^{2+}
Control (no additives)	10.96	8.52	0.510	50.5%
1% vol. glycerol	10.90	8.43	0.561	55.5%
1% vol. EG	10.98	8.26	0.558	55.2%
1% vol. MeOH	10.17	7.89	0.649	64.3%
1% vol. iPrOH	10.16	7.57	0.790	78.2%
1% wt. pentaerythritol	10.11	8.20	0.561	55.5%
1% wt. NPG	10.09	7.43	0.800	79.2%

formation of interactions between the molecules of the organic additive and the molecules of ammonia. Furthermore, all the additives used show a greater reduction rate of NH_3 escape during carbonate precipitation in post-distillation liquid than during absorption in an aqueous solution (Table 2). The highest percentage reduction was achieved with the use of neopentyl glycol (39.1% for absorption, 83.1% for precipitation). Glycerol and penthaerythritol also have a strong ability to reduce ammonia escape from the solution during precipitation (reduction of about 81%); however, glycerol works much worse in the case of CO_2 absorption in NH_3 aqueous solution (reduction of about 8%). Generally, it can be seen that no effect of organic additive on final ammonia concentration in solutions obtained after CO_2 absorption in the NH_3-H_2O solution, as well as in NH_3-$CaCl_2$-NaCl-H_2O solutions (Fig. 4). This is due to the mechanism of action of organic additives that interact with ammonia, and these interactions dominate over the salting-out effect.

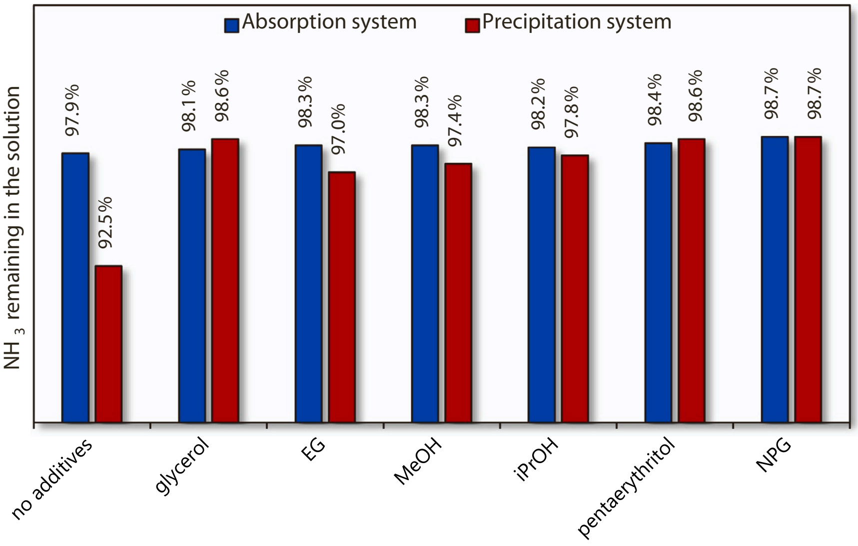

Fig. 4. Bar graph presenting the amount of NH_3 remaining in solution after the absorption and precipitation process depends on the additive used.

On the other hand, when comparing the results obtained for the NH_3-H_2O solution and the NH_3-$CaCl_2$-NaCl-H_2O solution without organic additives, the salting-out effects are visible and the concentration of ammonia in the solution containing salts decreased significantly.

3.3. CO_2 capture efficiency

The solubility of CO_2 in water is significantly reduced in the presence of dissolved inorganic salts [42,43]. This is due to an increase in the ionic strength, which increases the viscosity and density of the solution [43]. Thus, a higher escape of CO_2 is to be expected for absorption of CO_2 in post-distillation liquid (1.01 M $CaCl_2$, 0.966 M NaCl) than for absorption in aqueous solution, and this can be seen in the results obtained (Table 3), both for the process with and without additives used. The CO_2 capture efficiency (α) was determined using Eq. (9), with results obtained presented in Table 3.

$$\alpha = \frac{n_{in} - n_{out}}{n_{in}} \bullet 100\% \tag{9}$$

where n_{in} and n_{out} is a total number of CO_2 moles in the inlet and outlet stream, respectively. The highest CO_2 capture efficiency during precipitation was observed with neopenthyl glycol (86.1%) in this study. In comparison, the addition of isopropanol results in the achievement of a very similar value of CO_2 capture efficiency during precipitation (85%), but a much higher value of this parameter in the case of absorption in an aqueous solution (94.6%). Among the substances used as additives, both in the case of absorption in aqueous ammonia solution and in the carbonation process, monohydric alcohols appear to be better CO_2 capture enhancer than most tested polyols. This seems to be in agreement with the solubility of CO_2 in alcohols [44,45]. The addition of alcohols was suggested to have a chemical effect on the aqueous solution by decreasing the solubility of $CaCO_3$, and thus leading to increased supersaturation tendency [33]. As such, alcohol-water mixture solvents are very often used in $CaCO_3$ precipitation process. Furthermore, the addition of methanol and isopropanol can facilitate the transport of CO_2 from the gas phase to the liquid phase. It was found that methanol increases the CO_2 partitioning into the aqueous phase [46], while the presence of isopropanol in the aqueous solution results in the acceleration of CO_2 absorption during bubbling of the gas phase through the liquid phase, due to the formation of smaller gas bubbles in a solution with reduced surface tension [47].

3.4. The Ca^{2+} consumption during precipitation

Based on the titration results, the percentage consumption of calcium ions ($\%Ca^{2+}$) was determined using Eq. (10):

$$\%Ca^{2+} = \frac{[Ca^{2+}]_i - [Ca^{2+}]_f}{[Ca^{2+}]_i} \bullet 100\% \tag{10}$$

where $[Ca^{2+}]_i$ and $[Ca^{2+}]_f$ are initial and final calcium ions concentration in reaction mixture, respectively. Calculated calcium ions consumption, the initial and final pH of the reaction mixtures are shown in Table 4. The percentage of calcium ion consumption is directly related to CO_2 sequestration (Fig. 5). This is because the CO_2 that is absorbed in the solution can react with the calcium ions present in the mixture, leading to the precipitation of calcium carbonate. Thus, the higher the CO_2 capture efficiency, the higher the Ca^{2+} consumption; and the highest consumption of calcium ions was obtained during precipitation with the addition of neopentyl glycol. A very similar high value of this parameter was also achieved in the case of isopropanol.

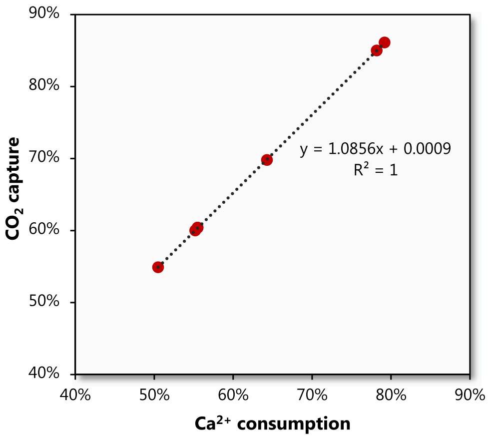

Fig. 5. Cross plot of the percentage of calcium ion consumption and CO_2 sequestration.

The X-ray diffractograms of all obtained samples (Fig. 6) confirms that calcium carbonate has been precipitated as a result of all conducted processes. Percentage content of vaterite (X_V) was calculated using the Eq. (11) based on the XRD results [48,49]:

$$X_V = \frac{7.691 \quad (I_V^{110})}{I_C^{104} + 7.691 \quad (I_V^{110})} \tag{11}$$

where I_C^{104} is the intensity of the calcite peak of the 104 plane and the I_V^{110} is the intensity of the vaterite peak of the 110 plane. All obtained $CaCO_3$ samples, regardless of additive used or not, are mainly in vaterite form (Table 5). The highest amount of vaterite (98.5%) was obtained during precipitation with the use of neopentyl glycol that also afforded the highest yield of $CaCO_3$ precipitation. This is consistent with the previous studies indicating that the formation of vaterite is much faster than that of calcite [50].

3.5. Interactions and hydrogen bonding

To gain a better understanding of the effect of the alcohols investigated, molecular-based thermodynamic modeling studies were performed to model possible interactions between the various additive molecules and different species that react during the processes. Specifically, possible competition among NH_4^+ ions, NH_3 and H_2O molecules to bond with the -OH groups of the alcohols was investigated in detail. The calculated energy effects for all considered alcohols when they form a single hydrogen bond with a single -OH group are shown in Fig. 7.

All tested organic additives can preferentially form hydrogen bonds with NH_3 molecules over water and ammonium ions as shown by the larger negative gain of energy (Fig. 7), which confirms their capability as NH_3 escape inhibitors; however, no direct correlation between energy gain and per-mole NH_3 capture could be observed. On the other hand, such correlation is visible if one considers the energy gain difference between NH_3 and NH_4^+ binding. As shown in Fig. 8, compounds that show a higher preference to bind free ammonia over its ionic form generally perform better in the real process, especially during the precipitation of $CaCO_3$ that shows the highest loss of NH_3 when no additives were used (Table 2). In this regard, it might be reasoned that the NH_3 capture efficiency depends mainly on the preference to bind NH_3 over other species, rather than the energy gain of the ROH-NH_3 bonding itself. In this case, comparing the NH_3/NH_4^+ energies seems to illustrate these differences better.

On the other hand, this approach does not correlate with the efficiency of CO_2 capture. However, it can be seen that the only two agents that provide significant CO_2 capture, isopropanol and neopentyl glycol, are also the only ones that do not show preference to bind NH_4^+ over H_2O. Since CO_2 actually reacts with NH_4^+ to form ammonium carbamate, it is quite reasonable that limiting NH_4^+ bonding with ROH should promote further CO_2 capture. Therefore, during CO_2 absorption, the influence of the reaction equilibrium (6) is not the dominant factor, and other system properties, such as solubility, mass transport rate, also influence

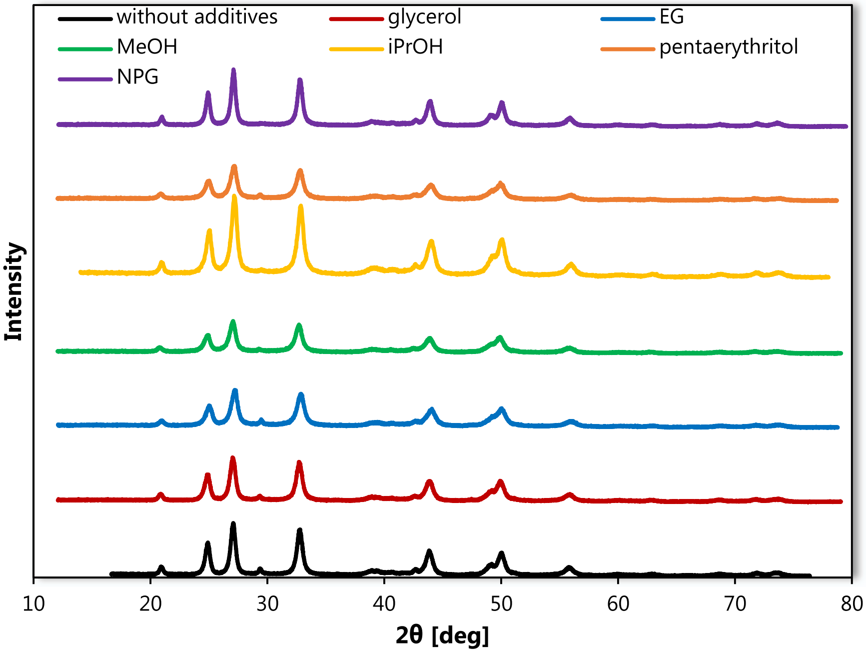

Fig. 6. XRD diffractograms of precipitated $CaCO_3$ samples.

Table 5
Percentage content of vaterite in precipitated samples (X_V).

Sample	X_V [%]
Control	96.7
1% vol. glycerol	96.8
1% vol. EG	96.7
1% vol. MeOH	97.1
1% vol. iPrOH	97.1
1% wt. pentaerythritol	96.7
1% wt. NPG	98.5

CO_2 capture.

Finally, it is also observed that polyols do not necessarily perform better as capturing agents for both NH_3 and CO_2 compared to e.g. isopropanol. This is especially clear for ethylene glycol and glycerol that have a more ‘dense’ distribution of -OH groups in their molecular structures. In such a case, it could be especially expected that the bonding molecule will not interact with only a single, but multiple –OH groups of the polyol. In order to verify the influence of bond formation with a higher number of –OH groups of ethylene glycol, glycerol and pentaerythritol, further calculations of the binding energy of NH_3 molecules and NH^{4+} ions were performed. The simulation results revealed that interactions of NH_3 and/or NH_4^+ with the second –OH group in the polyol molecules can further decrease their energy level; however, the second bonding is more favored for NH_4^+ than NH_3, as shown in Fig. 9 for pentaerythritol. The formation of the second H-bond can readily take place for NH_4^+, whereas the NH_3 molecule is too distanced from the second –OH group for the formation of a second H-bond. Similar simulation results were obtained for all the tested polyols, with the exception of the neopentyl glycol because of the long separation distance between both –OH groups.

In summary, molecular-based thermodynamic modeling results on the strength of H-bonds formed between the –OH groups and ammonia

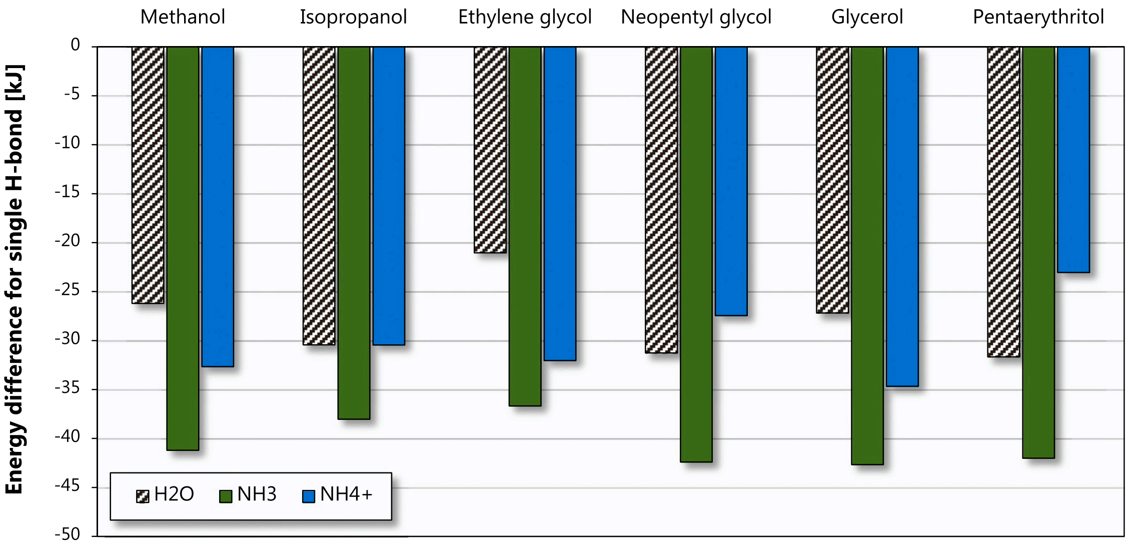

Fig. 7. Energy effect of H-bonding between studied alcohols and different molecules present during the processes.

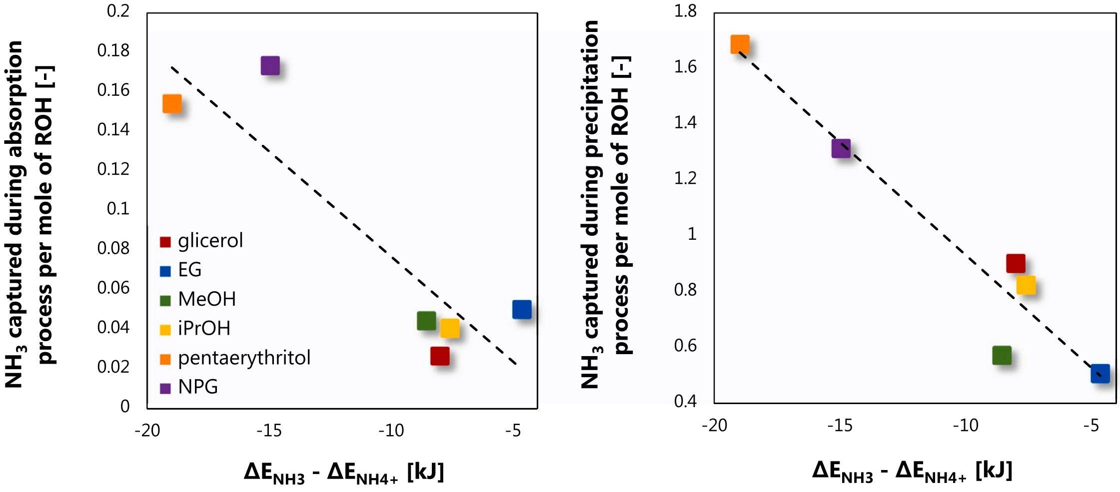

Fig. 8. Correlation between competition of NH_3/NH_4^+ bonding to alcohol and NH_3 captured during the absorption and precipitation processes.

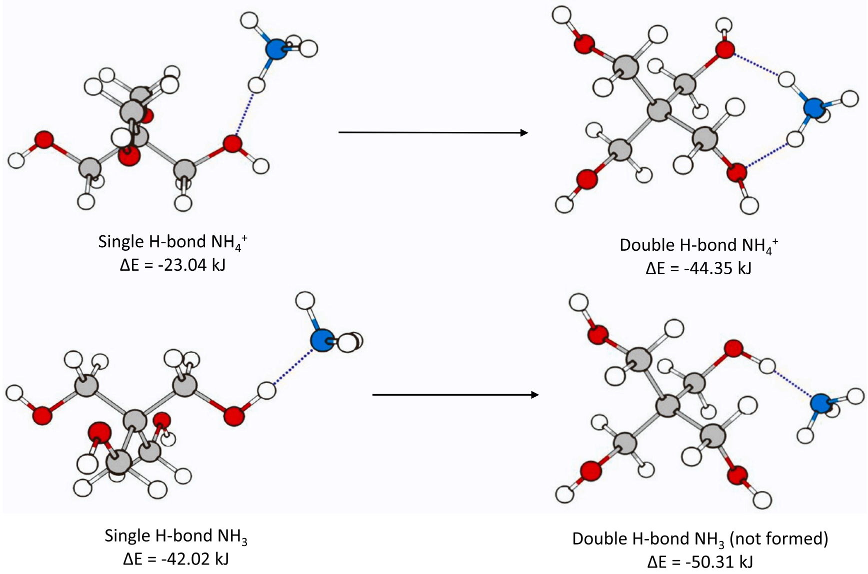

Fig. 9. Optimized geometries and energy effects of single double H-bonded NH_4^+ and NH_3 molecules with the pentaerythritol. Carbon, hydrogen, oxygen and nitrogen are grey, white, red and blue spheres, respectively.

and ammonium ions revealed the key features of molecules of various alcohols and polyols that influence their efficiency in the capture of ammonia in aqueous solutions. A strong preference to bind NH_3 is desirable for the ideal additive, while simultaneous bonding with NH_4^+ should be as limited as possible. In addition, an increasing number of –OH groups in additives can generally promote capture efficiency. Furthermore, the distance between neighboring –OH groups in the additive molecule is also important, and a closer location of these groups in the molecule favors the formation of dual bonds more with NH_4^+ than NH_3. The modeling results support the experimental observations that neopentyl glycol is the best additive for the NH_3/CO_2 capture efficiency among the studied alcohols and polyols.

4. Conclusions

In this study, the influence of selected organic substances containing hydroxyl groups on the reduction of ammonia escape and the improvement in CO_2 capture efficiency during the calcium carbonate precipitation by carbonation method using the post-distillation liquid from the Solvay process and the gas stream containing CO_2 in the amount corresponding to the exhausted gases produced by fossil fuel combustion was investigated. Two monohydric alcohols (methanol and isopropanol) and four polyols (ethylene glycol, neopentyl glycol, glycerol, and pentaerythritol) were tested as additives. Furthermore, during the proposed $CaCO_3$ precipitation using a post-distillation solution from the Solvay process and ammonia as the CO_2 absorption promoter, 98.7% of the NH_3 initially introduced into the reaction mixture remains in the solution. Among the tested additives, neopentyl glycol showed the highest reduction in NH_3 escape (83.1%) and the highest CO_2 capture efficiency (86.1%). The advantage of using NPG as an additive during $CaCO_3$ precipitation is obtaining the final product mainly in the form of vaterite (98.5%), which expands the possibilities for the potential use of this valuable by-product. Moreover, neopentyl glycol is nontoxic and nonvolatile, so it can be successfully used as an effective ammonia escape inhibitor in the proposed method of carbonation of the post-distillation liquid from the Solvay process.

Molecular-based thermodynamic modeling revealed the features of molecules that should be taken into account when introducing various alcohols and polyols to capture NH_3 and CO_2 in the calcium carbonate precipitation by carbonation method. It was shown that (i) a correlationship exists between the amount of ammonia retained and the H-binding energy of NH_3 and NH_4^+ with organic molecules, and (ii) increasing the number of -OH groups might promote capture efficiency. The modeling results provide further support for the carbonate precipitation experiments showing best capture efficiency of ammonia and carbon dioxide for solutions containing neopentyl glycol having two isolated hydroxyl groups in the molecule.

CRediT authorship contribution statement

Czaplicka Natalia: Conceptualization, Methodology, Investigation, Data curation, Visualization, Writing – original draft preparation. **Dobrzyniewski Dominik:** Methodology, Investigation, Data curation. **Szymon Dudziak:** Investigation, Visualization, Data curation. **Chunqing Jiang:** Writing – original draft preparation, Writing – review & editing. **Konopacka-Łyskawa Donata:** Conceptualization, Writing – review & editing, Supervision, Funding acquisition.

Declaration of Competing Interest

The authors declare that they have no known competing financial interests or personal relationships that could have appeared to influence the work reported in this paper.

Appendix A. Supporting information

Supplementary data associated with this article can be found in the online version at doi:10.1016/j.jcou.2022.102085.

References

[1] A.W. Zimmermann, J. Wunderlich, L. Müller, G.A. Buchner, A. Marxen, S. Michailos, K. Armstrong, H. Naims, S. McCord, P. Styring, V. Sick, R. Schomäcker, Techno-economic assessment guidelines for CO_2 utilization, Front. Energy Res. 8 (2020) 1–23, https://doi.org/10.3389/fenrg.2020.00005.

[2] Q. Wang, J. Luo, Z. Zhong, A. Borgna, CO_2 capture by solid adsorbents and their applications: Current status and new trends, Energy Environ. Sci. 4 (2011) 42–55, https://doi.org/10.1039/c0ee00064g.

[3] R.M. Cuéllar-Franca, A. Azapagic, Carbon capture, storage and utilisation technologies: A critical analysis and comparison of their life cycle environmental impacts, J. CO2 Util. 9 (2015) 82–102, https://doi.org/10.1016/j.jcou.2014.12.001.

[4] S. Snæbjörnsdóttir, F. Wiese, T. Fridriksson, H. Ármansson, G.M. Einarsson, S. R. Gislason, CO_2 storage potential of basaltic rocks in Iceland and the oceanic Ridges, Energy Procedia 63 (2014) 4585–4600, https://doi.org/10.1016/j.egypro.2014.11.491.

[5] P. Kelemen, S.M. Benson, H. Pilorgé, P. Psarras, J. Wilcox, An Overview of the Status and Challenges of CO_2 Storage in Minerals and Geological Formations, Front. Clim. 1 (2019) 1–20, https://doi.org/10.3389/fclim.2019.00009.

[6] D.S. Goll, P. Ciais, T. Amann, W. Buermann, J. Chang, S. Eker, J. Hartmann, I. Janssens, W. Li, M. Obersteiner, J. Penuelas, K. Tanaka, S. Vicca, Potential CO_2 removal from enhanced weathering by ecosystem responses to powdered rock, Nat. Geosci. 14 (2021) 545–549, https://doi.org/10.1038/s41561-021-00798-x.

[7] C. Gao, Y. Dong, H. Zhang, J. Zhang, Utilization of distiller waste and residual mother liquor to prepare precipitated calcium carbonate, J. Clean. Prod. 15 (2007) 1419–1425, https://doi.org/10.1016/j.jclepro.2006.06.024.

[8] M.S. Reid, X. Wang, N. Utting, C. Jiang, M.S. Reid, X. Wang, N. Utting, C. Jiang, GEOLOGICAL SURVEY OF CANADA OPEN FILE 8852 Comparison of water chemistry of hydraulic-fracturing flowback water from two geological locations at the Duvernay Formation. OPEN FILE 8852 Comparison of water chemi, GEOLOGICAL SURVEY OF CANADA,, Alberta, Canada, 2021.

[9] J. Fajfer, O. Lipińska, M. Konieczyńska, Hydraulic fracturing flowback chemical composition diversity as a factor determining possibilities of its management, Environ. Sci. Pollut. Res. 29 (2022) 16152–16175, https://doi.org/10.1007/s11356-021-16432-7.

[10] T. Kasikowski, R. Buczkowski, E. Lemanowska, Cleaner production in the ammonia-soda industry: An ecological and economic study, J. Environ. Manag. 73 (2004) 339–356, https://doi.org/10.1016/j.jenvman.2004.08.001.

[11] G. Steinhauser, Cleaner production in the Solvay Process: general strategies and recent developments, J. Clean. Prod. 16 (2008) 833–841, https://doi.org/10.1016/j.jclepro.2007.04.005.

[12] N. Czaplicka, D. Konopacka-Łyskawa, Utilization of gaseous carbon dioxide and industrial ca-rich waste for calcium carbonate precipitation: A review, Energies 13 (2020) 7–14, https://doi.org/10.3390/en13236239.

[13] R. Chang, S. Kim, S. Lee, S. Choi, M. Kim, Y. Park, Calcium carbonate precipitation for CO 2 storage and utilization: A review of the carbonate crystallization and polymorphism, Front. Energy Res. 5 (2017) 1–12, https://doi.org/10.3389/fenrg.2017.00017.

[14] G. Puxty, R. Rowland, M. Attalla, Comparison of the rate of CO_2 absorption into aqueous ammonia and monoethanolamine, Chem. Eng. Sci. 65 (2010) 915–922, https://doi.org/10.1016/j.ces.2009.09.042.

[15] P. Luis, Use of monoethanolamine (MEA) for CO_2 capture in a global scenario: Consequences and alternatives, Desalination 380 (2016) 93–99, https://doi.org/10.1016/j.desal.2015.08.004.

[16] D. Gonzalez-Garza, R. Rivera-Tinoco, C. Bouallou, Comparison of ammonia, monoethanolamine, diethanolamine and methyldiethanolamine solvents to reduce CO_2 greenhouse gas emissions, Chem. Eng. Trans. 18 (2009) 279–284, https://doi.org/10.3303/CET0918044.

[17] V. Darde, W.J.M. van Well, P.L. Fosboel, E.H. Stenby, K. Thomsen, Experimental measurement and modeling of the rate of absorption of carbon dioxide by aqueous ammonia, Int. J. Greenh. Gas. Control 5 (2011) 1149–1162, https://doi.org/10.1016/j.ijggc.2011.07.008.

[18] S. Ma, B. Zang, H. Song, G. Chen, J. Yang, Research on mass transfer of CO_2 absorption using ammonia solution in spray tower, Int. J. Heat. Mass Transf. 67 (2013) 696–703, https://doi.org/10.1016/j.ijheatmasstransfer.2013.08.090.

[19] Y.J. Kim, J.K. You, W.H. Hong, K.B. Yi, C.H. Ko, J.N. Kim, Characteristics of CO_2 absorption into aqueous ammonia, Sep. Sci. Technol. 43 (2008) 766–777, https://doi.org/10.1080/01496390701870606.

[20] J. Liu, S. Wang, B. Zhao, H. Tong, C. Chen, Absorption of carbon dioxide in aqueous ammonia, Energy Procedia 1 (2009) 933–940, https://doi.org/10.1016/j.egypro.2009.01.124.

[21] K. Li, H. Yu, G. Qi, P. Feron, M. Tade, J. Yu, S. Wang, Rate-based modelling of combined SO2 removal and NH3 recycling integrated with an aqueous NH3-based CO_2 capture process, Appl. Energy 148 (2015) 66–77, https://doi.org/10.1016/j.apenergy.2015.03.060.

[22] D.P. Hanak, C. Biliyok, V. Manovic, Efficiency improvements for the coal-fired power plant retrofit with CO_2 capture plant using chilled ammonia process, Appl. Energy 151 (2015) 258–272, https://doi.org/10.1016/j.apenergy.2015.04.059.

[23] F. Wang, J. Zhao, H. Miao, J. Zhao, H. Zhang, J. Yuan, J. Yan, Current status and challenges of the ammonia escape inhibition technologies in ammonia-based CO_2 capture process, Appl. Energy 230 (2018) 734–749, https://doi.org/10.1016/j.apenergy.2018.08.116.

[24] Y. Fangming, W. Yan, M. Lijuan, Study on the volatilization inhibition performance and mechanism of monolayer during the leakage process of ammonia solution, Can. J. Chem. Eng. 96 (2018) 704–711, https://doi.org/10.1002/cjce.22960.

[25] Z. Lv, T. Wang, K. Qiao, L. Yang, X. Du, Experimental study on carbon dioxide absorption by aqueous ammonia with nickel and chromium ions in bubbling tower at low temperatures, Chem. Eng. Res. Des. 179 (2022) 298–307, https://doi.org/10.1016/j.cherd.2022.01.035.

[26] N. Czaplicka, D. Konopacka-Łyskawa, B. Kościelska, M. Łapiński, Effect of selected ammonia escape inhibitors on carbon dioxide capture and utilization via calcium carbonate precipitation, J. CO2 Util. 42 (2020), https://doi.org/10.1016/j.jcou.2020.101298.

[27] J.K. You, H. Park, S.H. Yang, W.H. Hong, W. Shin, J.K. Kang, K.B. Yi, J.N. Kim, Influence of additives including amine and hydroxyl groups on aqueous ammonia absorbent for CO_2 capture, J. Phys. Chem. B. 112 (2008) 4323–4328, https://doi.org/10.1021/jp711113q.

[28] G. Pellegrini, R. Strube, G. Manfrida, Comparative study of chemical absorbents in postcombustion CO_2 capture, Energy 35 (2010) 851–857, https://doi.org/10.1016/j.energy.2009.08.011.

[29] J. Gao, Y. Zhang, D. Feng, Q. Du, M. Yu, M. Xie, L. Sun, S. Wu, A new technique of carbon capture by ammonia with the reinforced crystallization at low carbonized ratio and initial experimental research, Fuel Process. Technol. 135 (2015) 207–211, https://doi.org/10.1016/j.fuproc.2015.02.008.

[30] J.B. Seo, S. Bin Jeon, J.Y. Kim, G.W. Lee, J.H. Jung, K.J. Oh, Vaporization reduction characteristics of aqueous ammonia solutions by the addition of ethylene glycol, glycerol and glycine to the CO 2 absorption process, J. Environ. Sci. 24 (2012) 494–498, https://doi.org/10.1016/S1001-0742(11)60797-3.

[31] M.K. Kang, S. Bin Jeon, M.H. Lee, K.J. Oh, Improvement in CO_2 absorption and reduction of absorbent loss in aqueous NH3/triethanolamine/2-amino-2-methyl-1-propanol blends, Korean J. Chem. Eng. 30 (2013) 1171–1180, https://doi.org/10.1007/s11814-013-0072-1.

[32] M. Shuangchen, S. Huihui, Z. Bin, C. Gongda, Experimental study on additives inhibiting ammonia escape in carbon capture process using ammonia method, Chem. Eng. Res. Des. 91 (2013) 2775–2781, https://doi.org/10.1016/j.cherd.2013.05.015.

[33] S.F. Chen, S.H. Yu, J. Hang, F. Li, Y. Liu, Polymorph discrimination of CaCO3 mineral in an ethanol/water solution: Formation of complex vaterite superstructures and aragonite rods, Chem. Mater. 18 (2006) 115–122, https://doi.org/10.1021/cm0519028.

[34] F. Neese, The ORCA program system, Wiley Interdiscip. Rev. Comput. Mol. Sci. 2 (2012) 73–78, https://doi.org/10.1002/wcms.81.

[35] B. Zhao, Y. Su, W. Tao, L. Li, Y. Peng, Post-combustion CO 2 capture by aqueous ammonia: A state-of-the-art review, Int. J. Greenh. Gas. Control. 9 (2012) 355–371, https://doi.org/10.1016/j.ijggc.2012.05.006.

[36] B. Bossa, P. Theulé, F. Duvernay, F. Borget, T. Chiavassa, Carbamic acid and carbamate formation in NH3:CO_2 ices - UV irradiation versus thermal processes, in: Astron. Astrophys, 492, 2008, pp. 719–724, https://doi.org/10.1051/0004-6361:200810536.

[37] M. Shuangchen, S. Huihui, Z. Bin, C. Gongda, S. Zhu, Experimental study of Co(II) additive on ammonia escape in carbon capture using renewable ammonia, Chem. Eng. J. 234 (2013) 430–436, https://doi.org/10.1016/j.cej.2013.08.116.

[38] R. Beck, M. Seiersten, J.P. Andreassen, The constant composition method for crystallization of calcium carbonate at constant supersaturation, J. Cryst. Growth 380 (2013) 187–196, https://doi.org/10.1016/j.jcrysgro.2013.05.038.

[39] S. Ma, G. Chen, S. Zhu, T. Han, W. Yu, Mass transfer of ammonia escape and CO_2 absorption in CO_2 capture using ammonia solution in bubbling reactor, Appl. Energy 162 (2016) 354–362, https://doi.org/10.1016/j.apenergy.2015.10.089.

[40] R. Sing, B. Rumpf, G. Maurer, Solubility of ammonia in aqueous solutions of single electrolytes sodium chloride, sodium nitrate, sodium acetate, and sodium hydroxide, Ind. Eng. Chem. Res. 38 (1999) 2098–2109, https://doi.org/10.1021/ie980572g.

[41] E. Ruckenstein, I. Shulgin, Salting-out or -in by fluctuation theory, Ind. Eng. Chem. Res. 41 (2002) 4674–4680, https://doi.org/10.1021/ie020348y.

[42] W.A.G. Jones, S., Mass Transf. Chem. Precip. React. 46 (1991) 1027–1033.

[43] M. Görgényi, J. Dewulf, H. Van Langenhove, K. Héberger, Aqueous salting-out effect of inorganic cations and anions on non-electrolytes, Chemosphere 65 (2006) 802–810, https://doi.org/10.1016/j.chemosphere.2006.03.029.

[44] A.V.M. Nunes, G.V.S.M. Carrera, V. Najdanovic-Visak, M. Nunes Da Ponte, Solubility of CO_2 in glycerol at high pressures, Fluid Phase Equilib. 358 (2013) 105–107, https://doi.org/10.1016/j.fluid.2013.07.051.

[45] X. Gui, Z. Tang, W. Fei, Solubility of CO_2 in alcohols, glycols, ethers, and ketones at high pressures from (288.15 to 318.15) K, J. Chem. Eng. Data. 56 (2011) 2420–2429, https://doi.org/10.1021/je101344v.

[46] A.T. Kan, G. Fu, M.B. Tomson, Effect of methanol on carbonate equilibrium and calcite solubility in a gas/methanol/water/salt mixed system, Langmuir 18 (2002) 9713–9725, https://doi.org/10.1021/la025620n.

[47] D. Konopacka-Łyskawa, B. Kościelska, J. Karczewski, Eff. some Org. Solvent – Water mixtures Compos. precipitated Calcium Carbonate Carbon Process 418 (2015) 25–31, https://doi.org/10.1016/j.jcrysgro.2015.02.019.

[48] C.G. Kontoyannis, N.V. Vagenas, Calcium carbonate phase analysis using XRD and FT-Raman spectroscopy, Analyst 125 (2000) 251–255, https://doi.org/10.1039/a908609i.

[49] D. Konopacka-Łyskawa, N. Czaplicka, M. Łapiński, B. Kościelska, R. Bray, Precipitation and transformation of vaterite calcium carbonate in the presence of some organic solvents, in: Materials, 13, Basel,, 2020, pp. 1–14, https://doi.org/10.3390/ma13122742.

[50] J.D. Rodriguez-Blanco, S. Shaw, L.G. Benning, The kinetics and mechanisms of amorphous calcium carbonate (ACC) crystallization to calcite, via vaterite, Nanoscale 3 (2011) 265–271, https://doi.org/10.1039/c0nr00589d.